Hindawi
Advances in Polymer Technology
Volume 2020, Article ID 8749238, 8 pages
https://doi.org/10.1155/2020/8749238

Research Article

Synthesis of Polymer Assembled Mesoporous $CaCO_3$ Nanoparticles for Molecular Targeting and pH-Responsive Controlled Drug Release

Jinjing Xing, Yeqiang Cai, Yikun Wang, Haifu Zheng, and Yujia Liu

Jiangsu Institute of Metrology, Nanjing, Jiangsu 210023, China

Correspondence should be addressed to Jinjing Xing; xingganggang@sohu.com

Received 26 August 2019; Revised 22 October 2019; Accepted 31 October 2019; Published 5 January 2020

Guest Editor: Zhu Dong

$CaCO_3$ nanoparticles are very suitable as intelligent carriers because of their ideal biocompatibility and biodegradability, especially their sensitivity to pH. In this paper, we use mesoporous $CaCO_3$ nanoparticles as intelligent carrier, sodium alginate, and chitosan as alternating assembly materials, folic acid as target molecules, and exploit layer-by-layer assembly technology to achieve sensitive molecular targeting and pH response drug release. Mesoporous $CaCO_3$ hybrid nanoparticles have high drug loading on doxorubicin. The effects of different pH values on drug release in vitro were studied by regulating simulated body fluids with different pH values. The cytotoxicity, targeting effect, and drug release of human cervical cancer cell line (HeLa) were studied by cell vitality and imaging experiments. All the evidence suggests that the smart mesoporous $CaCO_3$ nanoparticles may be a potential clinical application platform for cancer therapy.

1. Introduction

In cancer treatment, because anticancer drugs alone cannot distinguish cancerous cells from healthy cells, serious side effects are almost inevitable [1–3]. In order to overcome these problems, a variety of intelligent drug delivery systems have been developed to improve the efficiency of drug delivery [4–6]. Various stimulation strategies, including light irradiation [7, 8], ion intensity [9, 10], redox potential [11], temperature [12], enzymology [13] and pH [14–17] have been developed for those drug delivery systems. Among them, pH response strategy has attracted special interest because of its ability to develop the acidic environment of cancerous tissues [18]. The pH value in tumor tissue (5.7–7.2) is lower than that in blood and normal tissue, and the pH value of endosome and lysosome is even lower (5.0–5.5) [19].

Calcium carbonate ($CaCO_3$) is an important biological mineral, which has attracted great attention in biomedical applications [20]. Compared with many other inorganic materials widely used in controlled transportation systems in the past, $CaCO_3$ nanosphere is very suitable as a non-toxic natural biological mineral because of its ideal biocompatibility, biodegradability and especially natural pH sensitivity [21–25]. So far, crystal $CaCO_3$ also shows promising potential for developing intelligent vectors for drugs, genes, and proteins [6, 26–31]. However, the previously developed $CaCO_3$ mixed particles are usually crystal solid spheres with smaller BET surfaces, and the larger BET surface area can greatly improve the ability to load drug molecules, regardless of their surface charge and hydrophilicity. The study of small particle size $CaCO_3$ mesoporous nanoparticles (MCNs) with nanometer mesoporous nanoparticles as drug carrier is rarely reported.

In recent years, layer-by-layer (LbL) technology based on alternating adsorption of charged substrate has remained attractive to fabricate pH responsive delivery because of its unique characteristics [22, 26, 31], including mild preparation conditions and easy customization (such as thickness, size and variable wall material). The targeted absorption of specific cells can also be realized by functionalizing the surface of the carrier by using biological targeting molecules (folic acid or antibodies, etc.) because it has mild manufacturing conditions and is easy to customize its characteristics [32, 33].

In this paper, the nanometer scale MCNs with pH responsive and molecular targeting functional as smart drug carriers were fabricated by the LbL self-assembly technique with sodium alginate (SA) and chitosan (CS) as the alternate

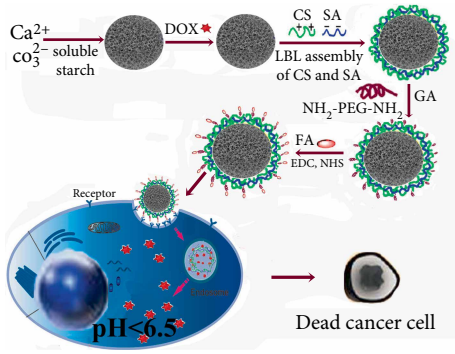

Figure 1: Molecular targeting and drug controlled release of mesoporous $CaCO_3$ nanoparticles assembled layer by layer.

assembling materials and surface modification with Polyethylene glycol (PEG) and targeting molecules (Figure 1), folic acid (FA), which is widely used as a specific targeting molecule for cancer cell [34–36]. The controlled release of drugs from mixed mesoporous $CaCO_3$ nanoparticles was studied in vitro by adjusting the simulated body fluids at different pH values. Cell vitality and imaging experiments were carried out to investigate the cytotoxicity, targeting and drug release effect of human cervical cancer cell line (HeLa).

2. Materials and Methods

2.1. Chemicals and Materials. $CaCl_2$, Na_2CO_3, Doxorubicin Hydrochloride (DOX) and soluble starch were obtained by Shanghai Aladdin reagent Co., Ltd, China. Chitosan (CS) was purchased by Golden-Shell Biochemical Co., Ltd. Zhejiang, China. Sodium alginate (SA) and glutaraldehyde (GA) were obtained from Shanghai Sangon. Biotech. Co. N-hydroxysuccinimide (NHS) and N-(3-dimethylaminopropyl)-N′-ethylcarbodiimide hydrochloride (EDC·HCl) were purchased from Sigma-Aldrich Co., Ltd. All chemicals were directly used as received without further purification. NH_2-PEG-NH_2 was purchased from Beijing Kaizheng Biological Engineering Development Co. Ltd. Millipore water (18.2 MΩ·cm at 25°C) was used throughout all of the experiments.

2.2. Preparation of Hierarchical Mesoporous $CaCO_3$ Nanoparticles (MCNs). Mesoporous $CaCO_3$ nanoparticles were prepared and then functionalized by LbL technique. In brief, using $CaCl_2$ (0.5 M), Na_2CO_3 (0.5 M) and soluble starch (5 wt%) as raw materials, $CaCl_2$ and soluble starch solution was prepared in a beaker and stirred for 30 min. Under strong stirring, Na_2CO_3 solution was injected into the mixed solution quickly. The system was stirred for 10 min, beakers were covered, rested for 24 hours, and then the product was collected by centrifugation. In this experiment, the final concentration of $CaCl_2$ and Na_2CO_3 was the same, and the final concentration of soluble starch was 1.25 wt%. The total volume of the reaction system is 400 mL.

2.3. Characterizations of MCNs. Transmission electron microscope (TEM) samples were prepared by dripping the samples dispersed in water into the carbon-coated copper gate evaporated by excess solvent. Tem images were recorded on JEOL JEM-1200 EX and the acceleration voltage was 100 kV. The surface analysis was carried out by ASAP 2020 adsorption analyzer at 77 K. The specific surface area is calculated by Brunauer-Emmett-Teller (BET) method and the pore size distribution is calculated by Barrett–Joyner Halenda (BJH) method. UV–vis spectra was obtained by Perkin Elmer Lambda 750 UV–vis spectrophotometer. Fourier transform infrared spectroscopy (FTIR) is provided by Nicolet Company of Nicolet Company.

2.4. DOX Loading into MCNs. Doxorubicin hydrochloric acid can be easily encapsulated in MCNs. The adsorption capacity of DOX-MCNs in hydrochloric acid solution (pH = 1) was determined at 486 nm. After DOX is unloaded in the medium, it can be directly used for the next batch of equivalent DOX. The drug loading and entrapment efficiency was calculated according to the following formula:

$$\text{Loading content}\left(\text{mg}\cdot\text{g}^{-1}\right) = \frac{\text{Quantum of drug in HCNs}}{\text{Quantum of HCNs loaded drug}}$$
$$\text{Entrapment efficient}\,(\%) = \frac{\text{Quantum of drug in HCNs}}{\text{Quantum mass of drug}} \times 100\%. \quad (1)$$

2.5. Layer-By-Layer Functionalized DOX-MCNs. The multilayer hybrid-coated mesoporous $CaCO_3$ nanoparticles were prepared by means of LBL assembly technique. The first step of the $CaCO_3$ nano-particle coating is to deposit a polyelectrolyte multilayer film (CS/SA/CS) on the $CaCO_3$ template. The outermost layer of the $CaCO_3$ nanoparticles is a cationic polyelectrolyte CS to positively charge the surface of the particles. The composite multilayer film was established by the electrostatic interaction between the negatively charged $CaCO_3$ nanoparticles and the polycation CS, and 200 mg of the $CaCO_3$ nanoparticles were dispersed in 40 mL of deionized water and 100 mg of CS was added for 1 h. And after three times of centrifugation and water washing, the CS, the deacetylation degree and the molecular weight are 96% and 6.0×10^5, are respectively deposited on the $CaCO_3$ nanoparticles to obtain the hybrid composite particles. The solution was then incubated for 60 min with 40 mL of SA (0.25% distilled water, viscosity 350 cps, 1 mg·mL^{-1} solution) and then centrifuged and dried. A multi-layer assembly consisting of 1 to 6 layers of CS/SA was prepared by continuous adsorption of two polyelectrolytes.

2.6. Folate-Conjugated DOX-MCNs. The surface of the mixed composite $CaCO_3$ nanoparticles was modified using bifunctional PEG. Briefly, about 200 mg of the above-prepared mixed composite $CaCO_3$ nanoparticles were dispersed in 25 mL of deionized water, and 1.5 mL of 1% glutaraldehyde (GA) was added to introduce the functional group. After the mixture was centrifuged and washed three times with water, 50 mg of NH_2-PEG-NH_2 was used with stirring at room temperature for 24 hours, and then 5 mL of sodium borohydride (2.0 mg· mL^{-1}) was added to the suspension. About 65 mg (0.15 mmol) of FA was dissolved in 2.5 mL of dimethyl sulfide oxide (DMSO).

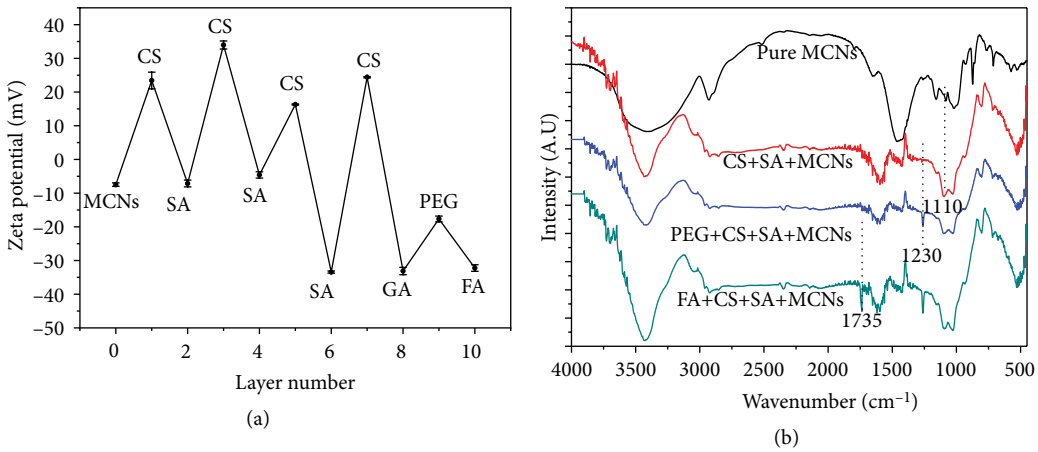

FIGURE 2: (a) Zeta potentials during the manufacturing process of the mesoporous $CaCO_3$ nano-particles assembled layer by layer. (MCNs: pure mesoporous $CaCO_3$ nanoparticles, CS: CS coating, SA: SA coating, GA: GA coating, PEG: PEG coating, FA: FA coating). (b) FT-IR spectra of different layer coating MCNs.

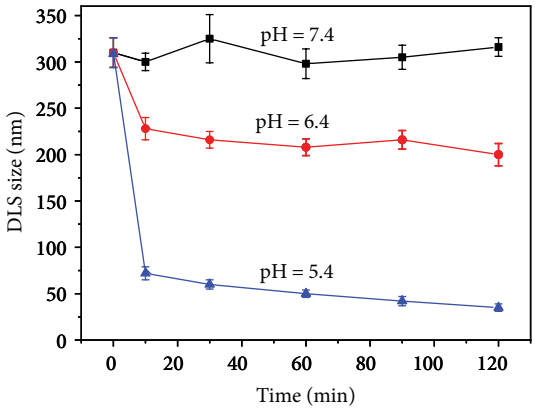

FIGURE 3: Time-dependent DLS-measurements of MCNS in PBS with different pH values (5.4, 6.4, and 7.4).

Then 40 mg of n-hydroxysuccinate (NHS) and 30 mg of N-(3-dimethylaminopropyl)-N-ethylcarbodiimide hydrochloride (EDC·HCl) was then added to the solution to activate the COOH group of the FA. The final molar ratio of FA/NHS/EDC was 1 : 2.2 : 1.1. The solution was then added to the suspension. After 24 hours, the free FA was removed by centrifugation and washed several times.

2.7. Size and Zeta Potential Measurements. The size and zeta potential of the prepared nanoparticles were measured by Zeta sizer (Nano ZS 90, Malven instrument). Before determination, deionized water (800 μL) was added to 200 μL solution containing nanoparticles for dilution. The data are mean ± standard deviation (SD).

2.8. In Vitro Controlled Drug Release. In vitro drug release experiment, 10 mg of folic acid conjugated and PEG modified DOX-MCNs powder were dispersed into 2 mL of deionized water. The dispersed solution was transferred to the dialysis bag (cut off molecular weight 7000), and then the bag was immersed in PBS solution of different 100 mL of pH (5.4, 6.4 and 7.4) at 37°C. At a certain interval, the solution of equal sample (1.0 mL) is taken, and then the same volume of fresh PBS solution is supplied. The amount of drugs released was measured by ultraviolet spectrophotometer.

2.9. Evaluation of In Vitro Cancer Cell Inhibition

2.9.1. MTT Assays. According to the previous report [37, 38], the cell viability of the functionalized DOX-MCNs mesoporous carrier was assessed using the MTT cell analysis. HeLa cells were cultured in DMEM supplemented with 10% fetal bovine serum (FBS), penicillin (100 units· mL^{-1}), streptomycin (100 mg·mL^{-1}) and 5% CO_2. The viability of the cells was analyzed using 3 [4,5-dimethyl-[2-based] 2,5-diphenyltetrabromobenzie (MTT, Sigma). The test was conducted in triplicate in the following manner, and the control experiment received without the MCNs vector and DOX was considered to be 100% growth. The cells were then incubated with DOX-loaded MCN with different concentrations, no drug MCN, and free DOX. About 1 mL of the complete medium and MTT (60 μL, 5 mg·mL^{-1}) were then added to each well and then incubated at 37°C for 4 hours, then the supernatant was carefully removed and 250 μL of DMSO was added to each well to dissolve the formazan crystals produced by viable cells. The absorbance of the solution was measured at 570 nm using a microplate reader (BioR550) to determine the OD value. The cell survival rate is calculated as follows:

$$\text{Cell viability}(\%) = \left(\frac{\text{OD}_{\text{treaded}} - \text{OD}_{\text{blank}}}{\text{OD}_{\text{control}} - \text{OD}_{\text{blank}}}\right) \times 100\%, \quad (2)$$

where the $\text{OD}_{\text{treated}}$ was obtained from cells treated with a specific reagent, the $\text{OD}_{\text{control}}$ was obtained from the cells without any treatment, and the OD_{blank} was obtained from only the culture and the reagent solution. Based on three independent measurements, the data is given as mean ± standard deviation (SD).

Table 1: DOX loading content and entrapment efficiency of the MCNs.

DOX/MCNs	Loading content ($mg \cdot g^{-1}$)	Entrapment efficiency (%)
0.1	38.5	82.3
0.3	52.4	85.3
0.6	83.6	75.3
0.8	108.9	73.2
1.0	110.4	73.0

2.9.2. Cell Imaging. In order to check the cell uptake and DOX release of the functionalized DOX-MCN, HeLa cells were cultured in a 12-well slider with a cover glass at the bottom of each chamber in a medium (DMEM) and incubated in cultured medium containing 200 $\mu g \cdot mL^{-1}$ of the nanocomposites at 37°C. After removal of the medium, the cells were washed three times with PBS (pH = 7.4) and the cover glass was observed under a laser scanning confocal microscope (TCSP5, Leica).

3. Results and Discussions

3.1. Characterization of Layer-By-Layer Assembled Hierarchical Mesoporous $CaCO_3$ Nanoparticles. The preparation and subsequent layer-by-layer assembly of layered mesoporous $CaCO_3$ nanoparticles are shown in Figure 2. Firstly, nano-sized mesoporous $CaCO_3$ nanoparticles were synthesized. The prepared MCNs exhibited a high surface area of 208 $m^2 \cdot g^{-1}$ and pore diameter of 11 nm as shown in Figure S1 (supporting information), indicating their mesoporous structure which may be helpful for the subsequent drug loading and controllable release.

LBL self-assembly technique was used to prepare coated multi-layer mixed nanoparticles by alternating adsorption of anion polyelectrolyte alginate (SA), cationic polyelectrolyte (CS) and anion layered MCNS by electrostatic interaction. The Zeta potential of the composite nanoparticles was carried out to track the polyelectrolyte multilayer coating, as shown in Figure 2(a). The Zeta potential of the pure prepared MCNs is −7.47 mV, and the negative charge on the surface of the nanoparticles is used as the hybrid anion in the process of LBL self-assembly. When the first layer of CS is deposited on the MCNs template, the zeta potential is about 23.43 mV, and the second layer of SA is −7.14 mV. It can be proved that the change of polyelectrolytes is adsorbed on the surface of MCNs template. We also note that when the number of layers of coated polyelectrolytes exceeds 5, the positive and negative potentials on the surface of nanoparticles are more than 20 mV. It is generally believed that the potential above the surface 20 mV will stabilize the nanoparticles in the solution, which indicates that polyelectrolyte deposition can improve the dispersion and stability in water [39, 40]. Considering that more polyelectrolyte (CS/SA) deposits induce larger hydrodynamic dimensions, five layers of polyelectrolytes are used as the best deposition and further research. When combined with functional NH_2-PEG-NH_2, the zeta potential of polyelectrolyte

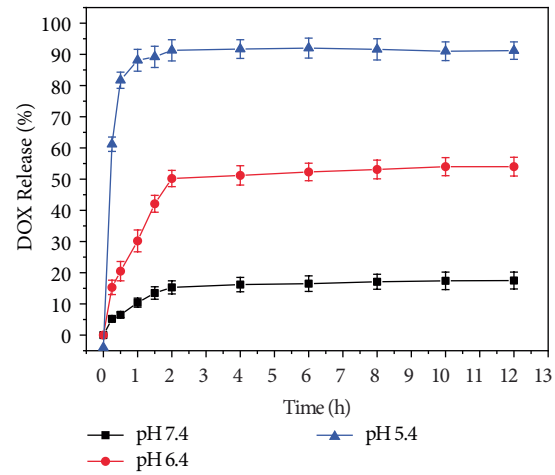

Figure 4: Time-dependent DOX release from the multiple layer coating MCNs in PBS with the different pH values.

mixed MCNs increased from −33.1 mV ($n = 3$) to −17.7 mV ($n = 3$), but decreased to −32.2 mV ($n = 3$) after FA was bound to the surface. The change of zeta potential was consistent with the binding of NH_2-PEG-NH_2 and FA, because NH_2-PEG-NH_2 was positively charged, while FA was negatively charged.

Figure 2(b) shows the Fourier transform infrared spectroscopy (FT-IR) of pure MCNs and different coating procedures. Compared with the MCNs prepared by SA, the FT-IR spectra of CS and SA functionalized MCNs have a new peak at 1110 cm^{-1}, which is related to the stretching vibration of C–O–C. In addition, a new peak of symmetrical tensile vibration of C-N appeared at 1230 cm^{-1}, which confirmed the successful functionalization of NH_2-PEG-NH_2 group. After grafting with FA, a new adsorption peak appeared at 1735 cm^{-1}, which could be attributed to the stretching vibration of C=O, indicating that the grafting of FA was successful.

The dynamic light scattering (DLS) data indicate that the hydrodynamic size of the multi-layer assemblied $CaCO_3$ (FA/PEG/SA/CS-MCNs) in the aqueous solution is about ~300 nm. In addition, its stability is evaluated by monitoring its hydrodynamic size in a complete cell culture medium containing 10% FBS, as shown in Figures S2, S3, S4 (support information). The dynamic size of the multi-layer coated MCNs did not change significantly within 96 h, indicating that these nanospheres were relatively stable in the biological fluid at physiological pH values, so that they were further applied in the biological system.

It is well known that the $CaCO_3$ can be decomposed in an acidic medium. The pH sensitivity of the multi-layer coating MCNs was tested by soaking in buffer at different pH values (5.4, 6.4, and 7.4). Under the condition of pH 7.4, the MCNs solution did not change significantly within 2 hours, whereas in the mild acid buffer of pH 6.4, the corresponding MCNs solution was gradually clear after 2 h, and more importantly, the MCNs solution was rapidly clear at pH 5.5, indicating the sensitive pH value responsibility of the nano-particles. In addition, the change of the hydrodynamic size of the nanoparticles with time at different pH, further confirmed the pH sensitivity of the DLS to the MCNs. As shown in Figure 3, the

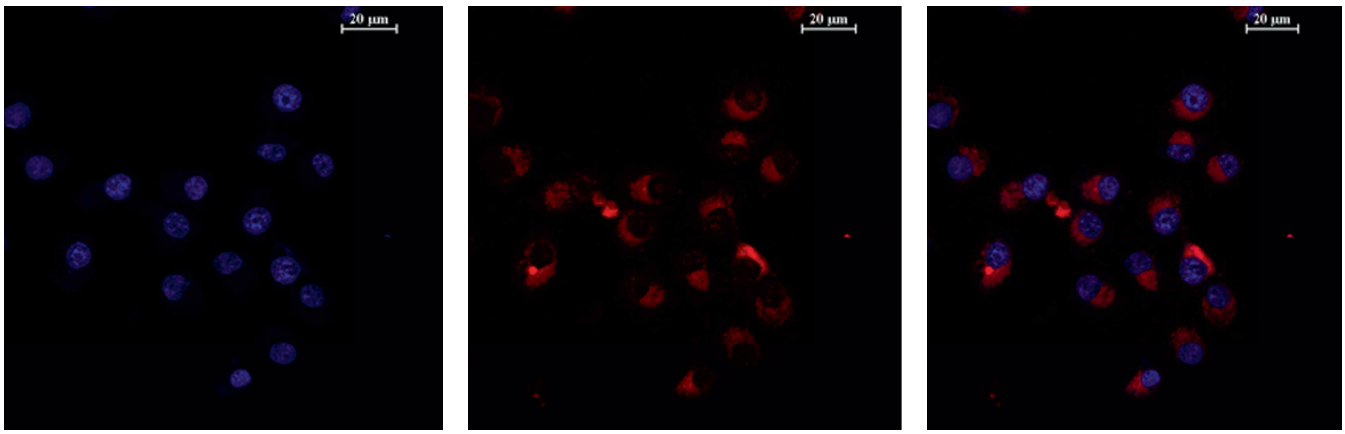

(a) (b) (c)

Figure 5: Confocal laser scanning microscope (CLSM) images of HeLa cells co-cultured with the prepared DOX-MCNs nanoparticles for 4 h. The left column (a) was Hoechst 33342 (blue) staining nucleus, the middle column (b) was DOX (red), and the right column (c) was a merged image from left column and middle column.

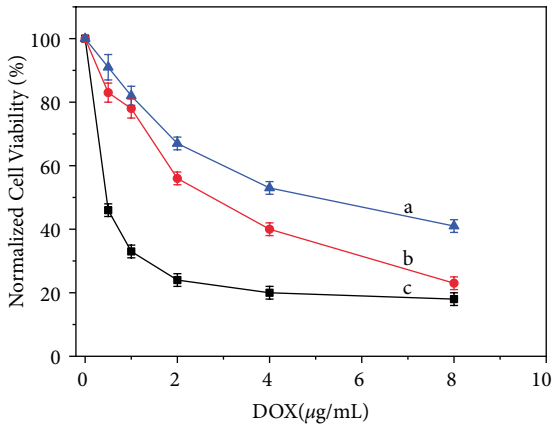

Figure 6: Cell viability of HeLa cells co-cultured with the free DOX (a) DOX-loaded hybrid MCNs modified with PEG (b) the DOX-loaded dual-targeting (FA) hybrid MCNs (c) for 48 h.

hydrodynamic size of the multi-layer coated MCNs dispersion buffer was not significantly changed under the condition of neutral pH 7.4, and the particle size of the nanoparticles decreased in a time-dependent manner at pH 6.4, indicating that the dissociation of the MCNs was slow, while at pH 5.4, the dissociation process was significantly accelerated.

3.2. High Drug Loading Efficiency. MCNs have a mesoporous structure and can be used for drug loading. Doxorubicin (DOX), a commonly used anticancer drug, was selected as the model drug and DOX was adsorbed on porous $CaCO_3$ nanoparticles. Table 1 shows that the DOX loading of MCNs increases rapidly with the increase of "DOX/MCNs" at different weight ratios of "DOX/MCNs", up to 108.9 $mg \cdot g^{-1}$ at "DOX/MCNs" = 0.8. The results showed that the carrier had a high drug loading on DOX.

3.3. DOX Release of the Multiple Layer Coating DOX-MCNs. The DOX release from the multi-layer coating DOX-MCNs at various pH values (5.4, 6.4, 7.4) was then measured, as shown in Figure 4. As expected, the release of DOX was significantly pH-dependent, no significant release was observed at a physiological pH (7.4) of 37°C, but under mild acid conditions, the drug was released from the carrier to a large amount of the external environment. The cumulative release of DOX can reach 92% at pH 5.5 after 2 h, which is much higher than that of pH 6.4 (50%) and 7.4 (13%), respectively.

3.4. Cellular Uptake. The feasibility of pH-responsive MCNs for DOX administration was evaluated with HeLa cells. As shown in Figure 5, strong red DOX fluorescence signals emerged inside cells after incubation with DOX-MCNs, suggesting the efficient cellular uptake of our nanoparticles. After 4 hours of co-culture, DOX was released from the vector and then concentrated rapidly in the nuclei region, consistent with previous reports [41, 42]. These results suggest that DOX-loaded MCNs can specifically respond to drug release in the pathological microenvironment in a pH response manner.

3.5. Targeting Function and In Vitro Cytotoxicity of the MCNs. In order to evaluate the FA-mediated targeting of polyelectrolytes (MCNs), the polyelectrolytes hybrid MCNs with FA-containing DOX loading and the DOX-loaded hybrid MCNs without FA were compared. As shown in Figure 6, the introduction of DOX results in a decrease in cell viability with the DOX concentration increases. In addition, the DOX-loaded FA-targeted polyelectrolytes hybrid MCNs exhibit a significant cell-inhibitory effect than only the PEG-modified MCNs, suggesting that this inhibition is mainly due to the acid-mediated targeting of the cells of the mesoporous microspheres [26, 27, 43].

The cytotoxicity of DOX loaded polyelectrolyte hybrid mesoporous nano-spheres in vitro was also studied in HeLa cells. Figure 7(a) shows the viability of HeLa cells incubated with different concentrations of functional MCNs within 24 hours. It was clearly observed that even after 72 hours, the viability of HeLa cells in all doses was as high as 91.0–102.5%,

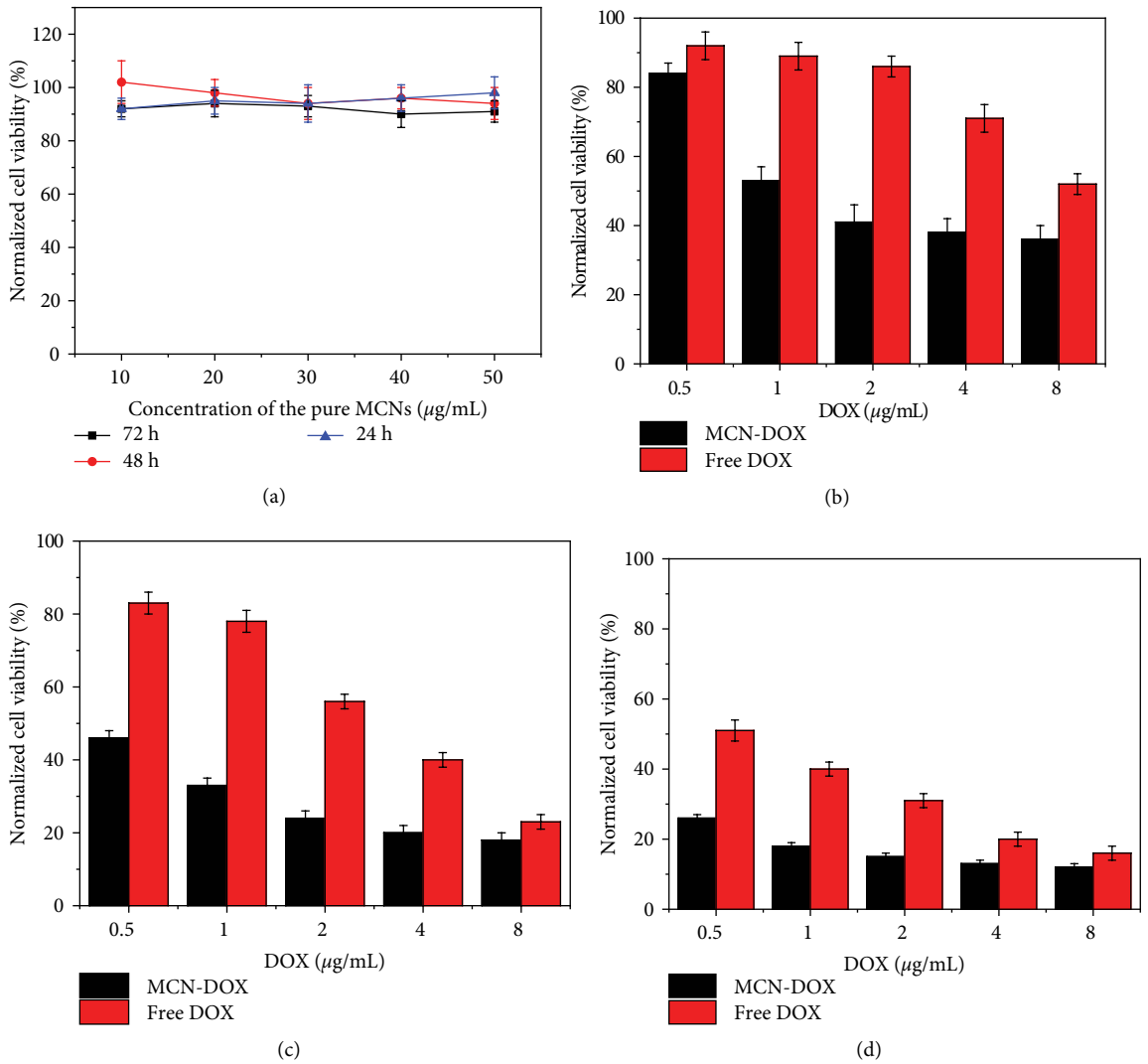

FIGURE 7: (a) Cell viability of HeLa cells co-cultured with the pure MCNs at the periods of 24–72 h and Cell viability of HeLa cells co-cultured with the free DOX and MCNs-DOX after 24 h (b), 48 h (c) and 72 h (d).

indicating that the multi-layer coated MCNs vectors without DOX drugs showed very low cytotoxicity. In the case of free DOX, the rapid insertion of DNA base pairs into nucleic acid [44, 45] resulted in cell killing (Figures 7(b)–7(d)). The pH response of DOX-MCNs after cell uptake determines the continuous killing effect in intracellular physiological environment. In addition, the cell activity treated with these nanoparticles showed typical time-dependent cell death (Figures 7(b)–7(d)).

4. Conclusion

In summary, we successfully developed a multifunctional nano-carrier with a pH response and a molecular targeting function, which is a single-dispersion nanoscale MCNs modified with the LBL self-assembly technology by using SA and CS as an alternative assembly material to target the molecular FA as a surface modifier. Under the physiological pH value of 7.4, the multi-layer coating MCNs-DOX is stable, while under the condition of micro-acid, the MCNs are rapidly degraded, resulting in the effective release of DOX. The nano-particles are co-cultured with HeLa cells, and the cell uptake efficiency is high, the cytotoxicity is low, and the molecular targeting property is strong. Considering the inherent biocompatibility and biodegradability of the $CaCO_3$, as well as the sensitive reaction to the pH value and the molecular target of the tumor, the prepared hybrid MCNs is a promising intelligent nano-drug delivery platform, and has a large clinical application prospect.

Data Availability

The data used to support the findings of this study are available from the corresponding author upon request.

Conflicts of Interest

The authors declare that there is no conflicts of interest regarding the publication of this paper.

Acknowledgments

We greatly appreciate the Jiangsu Institute of Metrology (JSIM, China) for the financial support (KJ175911).

Supplementary Materials

Supplementary materials include N_2 adsorption—desorption isotherms of prepared MCNs and dynamic light scattering (DLS) of multiple layer coating MCNs in DMEM + 10%FBS with different time. (*Supplementary Materials*)

References

[1] S. Bisht and A. Maitra, "Dextran-doxorubicin/chitosan nanoparticles for solid tumor therapy," *Nanomedicine and Nanobiotechnology* , vol. 1, no. 4, pp. 415–425, 2009.

[2] P. Duesberg, R. Li, R. Sachs, F. Alice, B. Up Madhvi, and H. Ruediger, "Cancer drug resistance: the central role of the karyotype," *Drug Resistance Updates*, vol. 10, no. 1-2, pp. 51–58, 2003.

[3] D. Zhu, H. M. Wen, W. Li, X. B. Cui, L. Ma, and A. Kang, "pH-responsive drug release from porous zinc sulfide nanospheres based on coordination bonding," *RSC Advances*, vol. 4, no. 63, pp. 33391–33398, 2014.

[4] T. M. Allen and P. R. Cullis, "Drug delivery systems: entering the mainstream," *Science*, vol. 303, pp. 1818–1822, 2004.

[5] C. Wang, Z. Li, D. Cao et al., "Stimulated release of size-selected cargos in succession from mesoporous silica nanoparticles," *Angewandte Chemie International Edition*, vol. 51, no. 22, pp. 5460–5465, 2012.

[6] Y. Zhao, Y. Lu, Y. Hu et al., "Synthesis of superparamagnetic $CaCO_3$ mesocrystals for multistage delivery in cancer therapy," *Small*, vol. 6, no. 21, pp. 2436–2442, 2010.

[7] T. D. Nguyen, K. C. F. Leung, M. Liong, Y. Liu, J. F. Stoddart, and J. I. Zink, "Versatile supramolecular nanovalves reconfigured for light activation," *Advanced Functional Materials*, vol. 17, no. 13, pp. 2101–2110, 2007.

[8] C. Park, K. Lee, and C. Kim, "Photoresponsive cyclodextrin-covered nanocontainers and their sol-gel transition Induced by molecular recognition," *Angewandte Chemie International Edition*, vol. 48, pp. 1275–1278, 2009.

[9] R. Casasus, E. Climent, M. D. Marcos et al., "Dual aperture control on pH- and anion-driven supramolecular nanoscopic hybrid gate-like ensembles," *Journal of the American Chemical Society*, vol. 130, no. 6, pp. 1903–1917, 2008.

[10] Y. Zhu, J. Shi, W. Shen et al., "Stimuli-responsive controlled drug release from a hollow mesoporous silica sphere/polyelectrolyte multilayer core-shell structure," *Angewandte Chemie International Edition*, vol. 44, no. 32, pp. 5083–5087, 2005.

[11] C. Y. Lai, B. G. Trewyn, D. M. Jeftinija et al., "A mesoporous silica nanosphere-based carrier system with chemically removable CdS nanoparticle caps for stimuli-responsive controlled release of neurotransmitters and drug molecules," *Journal of the American Chemical Society*, vol. 125, no. 15, pp. 4451–4459, 2003.

[12] Z. Zhou, S. Zhu, and D. Zhang, "Grafting of thermo-responsive polymer inside mesoporous silica with large pore size using ATRP and investigation of its use in drug release," *Journal of Materials Chemistry*, vol. 17, pp. 2428–2433, 2007.

[13] A. Schlossbauer, J. Kecht, and T. Bein, "Biotin-avidin as a protease-responsive cap system for controlled guest release from colloidal mesoporous silica," *Angewandte Chemie*, vol. 48, no. 17, pp. 3092–3095, 2009.

[14] C. H. Lee, L. W. Lo, C. Y. Mou, and C. S. Yang, "Synthesis and characterization of positive-charge functionalized mesoporous silica nanoparticles for oral drug delivery of an anti-inflammatory drug," *Advanced Functional Materials*, vol. 18, no. 20, pp. 3283–3292, 2008.

[15] C. B. Gao, H. Q. Zheng, L. Xing, M. H. Shu, and S. N. Che, "Designable coordination bonding in mesopores as a pH-responsive release system," *Chemistry of Materials*, vol. 22, no. 19, pp. 5437–5444, 2010.

[16] H. Q. Zheng, Y. Wang, and S. A. Che, "Coordination bonding-based mesoporous silica for pH-responsive anticancer drug doxorubicin delivery," *The Journal of Physical Chemistry C*, vol. 115, no. 34, pp. 16803–16813, 2011.

[17] H. Q. Zheng, C. B. Gao, B. W. Peng, M. H. Shu, and S. N. Che, "pH-responsive drug delivery system based on coordination bonding in a mesostructured surfactant/silica hybrid," *The Journal of Physical Chemistry C*, vol. 115, no. 15, pp. 7230–7237, 2011.

[18] K. C. F. Leung, C. P. Chak, C. M. Lo, W. Y. Wong, S. H. Xuan, and C. H. K. Cheng, "pH-Controllable Supramolecular Systems," *Chemistry—An Asian Journal*, vol. 4, no. 3, pp. 364–381, 2009.

[19] L. E. Gerweck, "Tumor pH: implications for treatment and novel drug design," *Seminars in Radiation Oncology—Journal*, vol. 8, no. 3, pp. 176–182, 1998.

[20] W. Wei, G. H. Ma, G. Hu et al., "Preparation of hierarchical hollow $CaCO_3$ particles and the application as anticancer drug carrier," *Journal of the American Chemical Society*, vol. 130, no. 47, pp. 15808–15810, 2008.

[21] Y. Guo, W. Jia, H. Li et al., "Facile green synthesis of calcium carbonate/folate porous hollow spheres for the targeted pH-responsive release of anticancer drugs," *Journal of Materials Chemistry B*, vol. 4, pp. 5650–5653, 2016.

[22] E. A. Genina, Y. I. Svenskaya, I. Yu Yanina et al., "*In vivo* optical monitoring of transcutaneous delivery of calcium carbonate microcontainers," *Biomedical Optics Express*, vol. 7, no. 6, pp. 2082–2087, 2016.

[23] G. Begum, T. N. Reddy, K. P. Kumar et al., "In situ strategy to encapsulate antibiotics in a bioinspired $CaCO_3$ structure enabling pH-sensitive drug release apt for therapeutic and imaging applications," *ACS Applied Materials & Interfaces*, vol. 8, no. 34, pp. 22056–22063, 2016.

[24] F. Kong, H. B. Zhang, X. Zhang et al., "Biodegradable photothermal and pH responsive calcium carbonate@phospholipid@acetalated dextran hybrid platform for advancing biomedical applications," *Advanced Functional Materials*, vol. 26, pp. 6158–6169, 2016.

[25] W. Feng, W. Nie, C. L. He et al., "Effect of pH-responsive alginate/chitosan multilayers coating on delivery efficiency, cellular uptake and biodistribution of mesoporous silica nanoparticles based nanocarriers," *ACS Applied Materials & Interfaces*, vol. 6, pp. 8447–8460, 2014.

[26] A. M. Yashchenok, M. Delcea, K. Videnova, and E. A. Jares-Erijman, "Enzyme reaction in the pores of $CaCO_3$ particles upon ultrasound disruption of attached substrate-filled

liposomes," *Angewandte Chemie International Edition*, vol. 49, pp. 8116–8120, 2010.

[27] D. B. Trushina, T. V. Bukreeva, and M. N. Antipina, "Size-controlled synthesis of vaterite calcium carbonate by the mixing method: aiming for nanosized particles," *Crystal Growth & Design*, vol. 16, pp. 1311–1319, 2016.

[28] B. V. Parakhonskiy, A. Haase, and R. Antolini, "Sub-micrometer vaterite containers: synthesis, substance loading, and release," *Angewandte Chemie*, vol. 124, pp. 1221–1223, 2012.

[29] A. Sergeeva, N. Feoktistova, V. Prokopovic, D. Gorin, and D. Volodkin, "Design of porous alginate hydrogels by sacrificial $CaCO_3$ templates: pore formation mechanism," *Advanced Materials Interfaces*, vol. 2, no. 18, Article ID 1500386, 2015.

[30] D. Zhao, C. J. Liu, R. X. Zhuo, and S. X. Cheng, "Alginate/$CaCO_3$ hybrid nanoparticles for efficient codelivery of antitumor gene and drug," *Molecular Pharmaceutics*, vol. 9, no. 10, pp. 2887–2893, 2012.

[31] Y. Zhao, Z. Luo, M. Li et al., "A preloaded amorphous Calcium Carbonate/Doxorubicin@Silica Nanoreactor for pH-responsive delivery of an anticancer drug," *Angewandte Chemie International Edition*, vol. 54, no. 3, pp. 919–922, 2015.

[32] P. M. Peiris, L. Bauer, R. Toy et al., "Enhanced delivery of chemotherapy to tumors using a multicomponent nanochain with radio-frequency-tunable drug release," *ACS Nano*, vol. 6, no. 5, pp. 4157–4168, 2012.

[33] S. Barua and S. Mitragotri, "Synergistic targeting of cell membrane, cytoplasm, and nucleus of cancer cells using rod-shaped nanoparticles," *ACS Nano*, vol. 7, no. 11, pp. 9558–9570, 2013.

[34] Z. Shen, Y. Li, K. Kohama, B. Oneill, and J. Bi, "Improved drug targeting of cancer cells by utilizing actively targetable folic acid-conjugated albumin nanospheres," *Pharmacological Research*, vol. 63, no. 1, pp. 51–58, 2011.

[35] M. Prabaharan, J. J. Grailer, S. Pilla, D. A. Steeber, and S. Q. Gong, "Folate-conjugated amphiphilic hyperbranched block copolymers based on Boltorn® H40, poly (l-lactide) and poly (ethylene glycol) for tumor-targeted drug delivery," *Biomaterials*, vol. 30, no. 16, pp. 3009–3019, 2009.

[36] C. Cortez, E. Tomaskovic-Crook, A. P. R. Johnston et al., "Influence of size, surface, cell line, and kinetic properties on the specific binding of A33 antigen-targeted multilayered particles and capsules to colorectal cancer cells," *ACS Nano*, vol. 1, pp. 93–102, 2007.

[37] J. Li, H. K. Jiang, X. O. Yang et al., "$CaCO_3$/tetraethylenepentamine–graphene hollow microspheres as biocompatible bone drug carriers for controlled release," *ACS Applied Materials & Interfaces*, vol. 8, no. 44, pp. 30027–30036, 2016.

[38] J. Leßig, B. Neu, and U. Reibetanz, "Influence of Layer-by-Layer (LbL) assembled $CaCO_3$-carriers on macrophage signaling cascades," *Biomacromolecules*, vol. 12, pp. 105–115, 2011.

[39] M. M. J. Kamphuis, A. P. R. Johnston, G. K. Such et al., "Targeting of cancer cells using click-functionalized polymer capsules," *Journal of the American Chemical Society*, vol. 132, no. 45, pp. 15881–15883, 2010.

[40] S. Munjal, N. Khare, C. Nehate, and V. Koul, "Water dispersible $CoFe_2O_4$ nanoparticles with improved colloidal stability for biomedical applications," *Journal of Magnetism and Magnetic Materials*, vol. 404, pp. 166–169, 2016.

[41] N. Sudareva, H. Popova, N. Saprykina, and S. Bronnikov, "Structural optimization of calcium carbonate cores as templates for protein encapsulation," *Journal of Microencapsulation*, vol. 31, no. 4, pp. 333–343, 2014.

[42] Z. L. Dong, L. Z. Feng, W. W. Zhu et al., "$CaCO_3$ nanoparticles as an ultra-sensitive tumor-pH-responsive nanoplatform enabling real-time drug release monitoring and cancer combination therapy," *Biomaterials*, vol. 110, pp. 60–70, 2016.

[43] E. C. R. Roti, S. K. Leisman, D. H. Abbott, and S. M. Salih, "Acute doxorubicin insult in the mouse ovary is cell-and follicle-type dependent," *PLoS One*, vol. 7, no. 8, p. e42293, 2012.

[44] G. H. Cheng, Y. M. Chai, J. Chen et al., "Polystyrene–divinylbenzene based nano-$CaCO_3$ composites for the efficient removal of human tumor necrosis factor-α," *Chemical Communications*, vol. 53, pp. 7744–7747, 2017.

[45] V. P. Parakhonskiy, A. Haase, and R. Antolini, "Sub-micrometer vaterite containers: synthesis, substance loading, and release," *Angewandte Chemie International Edition*, vol. 51, pp. 1195–1197, 2012.